

promoting access to White Rose research papers



Universities of Leeds, Sheffield and York
<http://eprints.whiterose.ac.uk/>

This is the author's version of an article published in **Bioresource Technology**

White Rose Research Online URL for this paper:

<http://eprints.whiterose.ac.uk/id/eprint/75978>

Published article:

Dou, B, Dupont, V, Williams, PT, Chen, H and Ding, Y (2009) *Thermogravimetric kinetics of crude glycerol*. *Bioresource Technology*, 100 (9). 2613 - 2620. ISSN 0960-8524

<http://dx.doi.org/10.1016/j.biortech.2008.11.037>

Thermogravimetric kinetics of crude glycerol

Binlin Dou, Valerie Dupont^{*}, Paul T. Williams, Haisheng Chen, Yulong Ding

School of Process, Environmental and Materials Engineering, University of Leeds, LS2 9JT,

UK

corresponding author: Dr Valerie Dupont

V.Dupont@leeds.ac.uk

Paper accepted and published. Full reference:

Binlin Dou, Valerie Dupont , Paul T. Williams, Haisheng Chen, Yulong Ding.

Thermogravimetric kinetics of crude glycerol . Bioresource Technology, 100 (2009) 2613-2620.

Thermogravimetric kinetics of crude glycerol

Binlin Dou, Valerie Dupont^{*}, Paul T. Williams, Haisheng Chen, Yulong Ding

School of Process, Environmental and Materials Engineering, University of Leeds, LS2 9JT,

UK

ABSTRACT

The pyrolysis of the crude glycerol from a biodiesel production plant was investigated by thermogravimetry coupled with Fourier transform infrared spectroscopy. The main gaseous products are discussed, and the thermogravimetric kinetics derived. There were four distinct phases in the pyrolysis process of the crude glycerol. The presence of water and methanol in the crude glycerol and responsible for the first decomposition phase, were shown to catalyse glycerol decomposition (second phase). Unlike the pure compound, crude glycerol decomposition below 500 K leaves behind a large mass fraction of pyrolysis residues (ca. 15%), which eventually partially eliminate in two phases upon reaching significantly higher temperatures (700 K and 970 K respectively). An improved iterative Coats-Redfern method was used to evaluate non-isothermal kinetic parameters in each phase. The latter were then utilized to model the decomposition behaviour in non-isothermal conditions. The power law model (first order) predicted accurately the main (second) and third phases in the pyrolysis of the crude glycerol. Differences of 10-30 kJ/mol in activation energies between crude and pure glycerol in their main decomposition phase corroborated the catalytic effect of water and methanol in the crude pyrolysis. The 3-D diffusion model more accurately reproduced the 4th (last) phase, whereas the short initial decomposition phase was poorly simulated despite correlation coefficients ca. 0.95-0.96. The kinetics of the 3rd and 4th decomposition phases, attributed to fatty acid methyl esters cracking and pyrolysis tarry residues, were sensitive to the heating rate.

Keywords: Biodiesel; by-product; glycerol; pyrolysis; TGA; FTIR; Kinetics

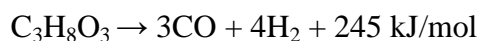
1. Introduction

Biodiesel has become more attractive recently as alternative diesel fuel to reduce dependency on fossil fuel imports. It is biodegradable, non-toxic, near CO₂-neutral and environmentally beneficial (Ma, et al., 1999). The transesterification of renewable biological sources such as vegetable oils and animal fat oils with an alcohol using alkaline or acid catalysts is the most common process for biodiesel production (Ma, et al., 1999 and Neyda, et al., 2008), yielding one mol of glycerol for every three of fatty acid methyl esters (FAME). With a production of biodiesel on the increase through the building of new bio-refineries worldwide, the crude glycerol by-product becomes a waste problem, and pure glycerol is in surplus (Adhikari^a, et al., 2007).

Crude glycerol from the biodiesel process often contains many impurities and is a very poor fuel, which is not used in either petrol or diesel engines (Slinn, et al., 2008). It can be purified by distillation to use in both food and pharmaceuticals or can be sent to water treatment for digestion. However, these processes are very expensive and exhibit a low yield (Slinn, et al., 2008). Several alternatives are being explored to utilise crude glycerol, and some commercial plants have been established to produce 1,3-propanediol, polyglycerols and polyurethanes from glycerol (Valliyappan, et al., 2008 and Adhikari, et al., 2008). One mol of glycerol (C₃H₅(OH)₃) can theoretically produce up to 4 mol of hydrogen gas, and in addition, it is possible to get CO as one of the gaseous products due to the high oxygen content. Glycerol as a potential feedstock via pyrolysis, gasification or steam reforming to produce H₂, CO or other fuel gases has received considerable research attention (Valliyappan, et al., 2008; Stein et al., 1983; Zhang et al., 2007; Dauenhauer et al., 2006; Czernik et al., 2002; Buhler et al., 2002; Aurelien et al., 2007; Sun et al., 2008; Ranjbar et al., 1991). In a previous study on hydrogen production from unmixed

steam reforming of sunflower oil fuels, the thermal decomposition of the fuel was found to play a significant role in the H₂ production and coke formation (Dupont et al., 2007). There are also many opportunities for liquid biofuels to pyrolyse upstream of a steam reforming catalyst during the consecutive stages of the process, from the fuel injection, evaporation, to the mixing and reacting of the vapourised fuel with the steam in the reformer. Understanding the pyrolysis of crude glycerol is therefore important to design steam reforming processes that avoid tar and coke formation.

The pyrolysis of glycerol without catalyst is a very simple and a cheap method for energy conversion. Stein et al. (1983) studied the pyrolysis of glycerol in steam in a laminar flow reactor. The initial products of decomposition were CO, acetaldehyde and acrolein, and then acetaldehyde and acrolein further decomposed to produce primarily CO, CH₄ and H₂. Valliyappan, et al. (2008) reported the hydrogen or syngas production from glycerol by pyrolysis at temperatures higher than 600°C and the products were mainly gases consisting of CO, H₂, CO₂, CH₄ and C₂H₄. The thermal decomposition of glycerol in near-critical and supercritical water was also carried out by Buhler et al. (2002) in a tubular reactor and a conversion between 0.4 and 31% was observed. They reported the main products of the glycerol degradation included methanol, acetaldehyde, ethanol, CO, CO₂ and H₂. The decomposition is highly endothermic for glycerol:



Due to high oxygen content, complex intermediates and high impurity levels, it is also very difficult to understand the characteristics of pyrolysis of the crude glycerol from the biodiesel production process. In this paper, following characterisation by GC-MS and CHNS analysis of crude glycerol from a biodiesel refinery, its pyrolysis was carried out in dry N₂ was studied by thermogravimetry coupled with Fourier transform infrared spectroscopy (TGA-FTIR). Other feedstocks such as pure glycerol, water/glycerol and methanol/glycerol mixtures were also

analysed in TGA experiments to obtain a better understanding of the crude glycerol decomposition behaviour.

The thermogravimetric experimental data were interpreted by an improved iterative Coats-Redfern method, which allows the kinetic parameters to be estimated iteratively by linear regression and thus enhances the accuracy (Urbanovici et al., 1999). A number of forms of the mechanism integral function $g(\alpha)$ were tested with the experimental data, including:

- (i) the power law model, $g(\alpha) = \alpha^{1/m}$, $m = 1, 2, 3, 4$
- (ii) the reaction order model $g(\alpha) = (1 - (1 - \alpha)^{1-n}) / (1 - n)$ with n the order of reaction
($g(\alpha) = \ln(1 - \alpha)$ when $n = 1$)
- (iii) 1D, 2D and 3D diffusion models (e.g. 3D: $g(\alpha) = (1 - (1 - \alpha)^{1/3})^2$)

The kinetics parameters were evaluated by minimizing the equation for the sum of the squares of residual errors (S_{res}) (Urbanovici et al., 1999), and the best model identified by its correlation coefficient's closeness to 1.

2. Experimental

2.1 Materials

The crude glycerol was obtained from D1-Oils Ltd, Middlesborough, UK. It mainly consisted of 70-90wt% glycerol compound based on the data sheet from Directive 2001/58/EC provided by the manufacturer. Other compounds listed by the manufacturer were methanol (<15%), water (<15%), inorganic salts (<5%) and polyglycerol (<5%). In order to reduce its viscosity and allow the crude glycerol to be pumped, the manufacturers usually dilute the crude phase with ca 10% water, the mixture can then be used as oil-fired in power plants. The sample investigated here had undergone such a procedure. The CHNS elemental composition of the

crude glycerol was determined for three samples using a CE Instrument Flash EA 1112 Series. The resulting average elemental molar formula was $C_{3 \pm 0.2}H_{8.9 \pm 0.4}O_{3.4 \pm 0.2}N_{(5 \pm 2) \times 10^{-3}}$, with the O content derived by difference from 1 of the sum of the measured C,H,N mass fractions. This indicates higher H/C and O/C ratio compared to pure glycerol ($C_3H_8O_3$). This would have been partly contributed by the presence of the H_2O and methanol (CH_3OH) content in the crude, unlike the fatty acid methyl esters impurities H/C and O/C ratios are lower than those of glycerol. Simple, non quantitative characterisation by GC/MS was carried out in this study using a Trace GC 2000 TOP (Thermo electron), with a splitless injector and a mass spectrometer Fisons MD800. The column used for GC is the $25m \times 0.25mm$ RESTEK RT and the helium of 1 ml/min was used as the carrier gas. The GC-MS analysis was performed with an oven temperature program from 333 to 583K at 5K/min and the solvent used to dissolve the crude glycerol was selected as methanol. The composition of crude glycerol varies depending on the plant oils or animal oils employed as primary source. The GC-MS spectrum obtained for the sample indicated the presence of glycerol $C_3H_5(OH)_3$, and of significant methyl esters products of the biodiesel process, among them, linoleic ($C_{19}H_{34}O_2$), palmitic ($C_{17}H_{34}O_2$), oleic ($C_{19}H_{36}O_2$), and stearic ($C_{19}H_{38}O_2$) acid methyl esters. With the aim of discussing some of the crude glycerol components contributions to its thermal degradation behaviour, pure glycerol and mixtures of 10% distilled water in glycerol and 10% methanol (99.5% purity) in glycerol, were subjected to similar thermal gravimetric experiments as the crude. The glycerol (99.1% purity) and the methanol (99.5% purity) were purchased from Sigma Aldrich.

2.2 TGA-FTIR studies

Thermogravimetry coupled with Fourier transform infrared spectroscopy (TGA-FTIR) experiments were carried out to study the pyrolysis of the crude glycerol. Thermogravimetric

data were collected from 300 K to 1123 K at the heating rates of 5, 10, 15, and 20 K/min, under dry nitrogen atmosphere by using a Stanton Redcroft TGA apparatus. For comparison, pure glycerol samples were also analysed at the same heating rates, while the 10% water-glycerol as well as 10% methanol-glycerol were analysed at the heating rate of 5 K/min in the TGA. Sample masses of about 20 mg were used. The pyrolysis products were carried through a stainless steel line into the gas cell for IR absorption detection. Both the transfer line and the gas cell were kept at 150 °C to prevent gas condensation although the less volatile gases such as vapours of some compounds with high boiling point were expected to condense partially in this line. IR spectra were obtained using a magna system 560 spectrometer with a resolution of 4 cm^{-1} averaging 100 scans in the wavenumber range of 4000-500 cm^{-1} and the detector is the DTGS KBr. Total data collection time was 70.25 min.

3. Results and discussion

3.1 Analysis of thermogravimetry

Figure 1 shows the TG mass loss curve of the pure glycerol with a 15 K/min heating rate and those of crude glycerol at various heating rates (5, 10, 15 and 20 K/min) in order to study the effect of heating rate on non-isothermal kinetics. As can be seen, the pyrolysis pattern of the crude glycerol at the different heating rates for each sample was similar, indicating four phases in the pyrolysis process. The mass loss, initial mass loss temperature, maximum mass loss temperature and final mass loss temperature for each phase in the pyrolysis of crude glycerol are shown in Table 1 for the four heating rates 5, 10, 15 and 20 K/min. Table 2 lists the same parameters for the pyrolysis of pure glycerol. The TG mass loss curve of the pure glycerol was simple and only presented one phase, covering 95% of its mass loss, spanning from (423-453) K

to (503-556) K depending on the heating rate. The decomposition of the pure glycerol was almost complete, leaving only 2% mass residue upon further heating. For the crude glycerol, the mass loss values during the first phase (PH1) were about 10-15% and spanned from (322-343) K to (426-440) K depending on the heating rate. The removal of water and some low temperature volatiles such as methanol, the co-reactant in the transesterification of vegetable oil were most likely responsible for this low temperature first phase of mass loss. The role of water and methanol during PH1 was corroborated by additional TGA experiments at 5 Kmin⁻¹ of the mixtures of 10% water in pure glycerol and of 10% methanol in pure glycerol, shown in Fig.2. Both of the 10% mixtures exhibited a 10% mass loss in the exact same temperature region as the crude glycerol during PH1. The main mass loss of crude glycerol pyrolysis occurred during the second phase (PH2) from (426-440) K to (501-548) K depending on the heating rates. The percentage of the mass loss during PH2 was about 67-69%. Some studies on the pyrolysis of the liquid nitrate esters by TGA showed the main loss of 98% between room temperature and 550K (Sun et al., 2008). Interestingly, we can see from Fig. 2 that for a given temperature in the main decomposition phase, the pure glycerol shows significantly higher remaining mass, hence lower mass loss, than the 10% mixtures and than the crude glycerol. This indicates that the pyrolysis of the glycerol in the crude mixture may be catalysed with similar effect by both the water and the methanol content in the crude. This will be explored further with the help of the kinetic analysis. Phase 3 of the crude glycerol extended from 501K to 774K depending on the heating rate, and accounted for 10.2 to 12.7 % of the crude glycerol mass. Given that the water and methanol content as well as 95% of the glycerol mass are expected to have been lost prior to PH3, it is expected that phase 3 (PH3) would have consisted in the thermal degradation of the impurities such as the fatty acid methyl esters and that of their residues from early degradation during PH2, forming further gases and leaving less residual matter. A final phase of crude glycerol pyrolysis (PH4), spanned from 760 to 1123 K, accounting for 3.7-5.8% mass loss

depending on heating rate. The final residual in the pyrolysis of crude glycerol at 1123K consisted of coke and ash, in amounts varying between 3.5 and 4.5 wt%, roughly twice as much as the pure glycerol final residue. It is known that the pyrolysis of glycerol, and fatty acid methyl esters producing coke may occur as a result of secondary reactions between the products of thermal cracking (Ranjbar and Pusch, 1991). The tendency for these potential steam reforming or partial oxidation feedstocks to produce coke is therefore a challenge given the reliance on catalysts that are carbon-deposition sensitive in such processes. It is important to design the processes so as to avoid coke formation from high temperature thermal degradation of crude glycerol compounds.

3.2 Analysis of FTIR

The evolution of gaseous species and products as a result of the pyrolysis of crude and pure glycerol samples was simultaneously monitored by FTIR during the TGA experiment at the heating rate of 15 K/min. The formation of the main gas components including CO₂, H₂O, CH₄, CO, H₂ and coke is summarised in (Valliyappan et al., 2008).

All the spectra show bands at 3636, 3724.4, 3853.2, 3948.1 and 1508.6 cm⁻¹ and could be attributed to O-H stretching from the water. The bands located at 2924 and 2842 cm⁻¹ were assigned to C-H vibrations of methyl and methylene groups. The bands related with C-O stretching were detected at 1102.6, 2184.7 and 2090.6 cm⁻¹. Some bands at 669.4, 2309.6, 2321.4, 2344.8 and 2351.2 cm⁻¹ were attributed to CO₂. The bands at 911.9 and 1733.4 cm⁻¹ may be attributed to C=C and C=O from carboxylic compounds.

Looking more closely at the individual phases of the crude glycerol pyrolysis, when reaching the end of phase 1, the absorbance spectrum at 402 K exhibited peaks attributable to CH₄, CO and H₂O, and no CO₂ absorbance peaks. This indicates that the glycerol component in

the crude began to decompose during PH1 and the initial reactions at relatively low temperature did not form CO₂. Early in PH2 (506K), in addition to the growing peaks attributable to H₂O, CO₂, CO, functional groups of C-H, C-O, C=O of aldehydes and esters were also detected. Increasing the temperature to 528 K corresponding to the middle of PH2, the absorption peaks of CO₂ grew stronger at 669.4, 2309.6-2351.2 cm⁻¹. The intensity of the CO₂ and H₂O greatly increased, while a CH₄ peak was still identified (2896.3 cm⁻¹), only the absorbance peak of C-O, appeared weakened. This confirms that during PH2, the main thermal decomposition reactions of glycerol occurred, and more gases were produced. Further heating to 739 K and 996 K corresponding to mid-PH3 and mid-PH4 the absorption peaks of CH₄ almost completely disappeared, and the intensities of the absorption peaks of C-O continued to weaken whereas the peak at 2184.7 cm⁻¹ of CO gas was the strongest at 739K. In these phases, the intensities of absorbance peaks of H₂O and CO₂ were still very strong. At the same time, there were absorbance peaks of C-C, C-O-C and in particular strong C=O stretching vibrations. These may be attributable mainly to the cracking of the fatty acid methyl esters and to the products of their decomposition as well as to a much lower expected extent, further decomposition products of the glycerol pyrolysis residue. Respective significance of the former over the latter is reflected by the differences in the TGA mass loss curves of the crude and pure glycerol above 530 K. It can be seen that with changing the temperature, the intensities of absorbance peaks of CH₄ reached its maximum during PH2. Interestingly, with CH₄ a major product of the crude glycerol decomposition in phase 2 (main decomposition phase), this may have adverse consequences when steam reforming of the crude glycerol, as catalytic methane steam reforming may require temperatures higher than pure glycerol catalytic steam reforming. In addition, no N- or S-containing compounds were detected and some gases such as H₂, N₂, and O₂ have no IR absorption or have very weak peaks, and so are undetectable by FTIR (Yan et al., 2005).

Some researchers studied that the concurrent and dehydration reactions of gas-phase pyrolysis of glycerol at low temperatures may lead to the formation of the products such as liquid, gas and char (Stein et al., 1983). At high temperatures, consecutive thermal cracking reactions were predominant to form H₂, CO, CO₂ and coke. Different pathways of these species formation can be presumed, via the formation of the intermediates acrolein (C₃H₄O) and acetaldehyde (C₂H₄O) (Stein et al., 1983 and Buhler et al., 2002). A simple H₂O-elimination and deprotonation from glycerol leads to acrolein. Acetaldehyde has been detected to nearly all temperature conditions in the TGA-FTIR of the present study, which may be formed by the primary protonated glycerol. Species such as formaldehyde (H₂CO), the formyl radical (HCO) and CH₂OO may undergo the decomposition to CO₂, CO H₂O and H₂ production at high temperature (Gao et al., 2008):

Some results indicated that as temperature increased, the production of H₂ increased and carbon deposited due to the cracking of some hydrocarbons (Valliyappan et al., 2008). Carbon formation may lead to blockage of catalyst pores in steam reforming and in extreme cases complete failure of the reactor. Some gasification reactions of carbon with H₂O, H₂, and CO₂ at high temperatures may avoid its production.

3.3 Kinetic analysis

A comparison of the models indicated that for the first three phases of the crude glycerol pyrolysis, the best fit was the power law ($m = 1$). Such a best fit was verified by (i) a linear correlation coefficient closer to 1 than the other models tested, (ii) close agreement in the conversions found experimentally and those recalculated with the derived kinetic parameters and the best fit model. The calculated conversions curves are compared with the experimental ones in Figs. 3-7. The kinetic parameters used to build these curves are listed in Tables 3 to 6 for

phases from PH1 to PH4 respectively. Also included in Tables 3-6 are the correlation coefficients, the number of data points used in the linear fit, and the range of conversions used to obtain them. In the calculations, the subroutine 'fitexy' of the numerical recipes (Press, et al., 1992) was used to find estimates of A and E , and to calculate their uncertainties based on an assumed error of 1% on both absolute temperature and conversions. The conversions were re-calculated as a function of temperature using these values of E and A and the best-fit mechanism integral function, effectively modelling the TGA experiment. In the construction of Figs. 3-5 corresponding to the kinetic modelling of PH2 and PH1, the conversion values used for the fit were those obtained using the extrema of sample masses from the full TGA run. In Figs. 6-7 corresponding to PH3 and PH4 respectively, the conversions used for the fits were normalised between 0 and 1, using the extrema of sample masses from the relevant phase only, as opposed to those of the full TGA run. Using conversions normalised between 0 and 1 for PH1 and PH2 failed to reproduce well the experimental results, and similarly, a non-normalised conversion approach in PH3 and PH4 did not yield good modelling results.

3.4 Individual discussion of each phase of crude glycerol decomposition

The lower values of the activation energy E in phase 1, found between 27 and 34.8 kJ/mol and shown in Table 3, confirmed that physical changes such as the evaporation of water and methanol and/or the breaking of the weak chemical bonds occurred during the first stage of the pyrolysis of crude glycerol. It is therefore difficult to attribute the activation energies or enthalpies of vaporisation derived for PH1 to particular components of the crude glycerol. This is reflected by the poor modelling fit obtained for PH1 conversions for all the heating rates studied (Fig. 5). PH1 and PH2 were not well reproduced by modelling when using normalisation between 0 and 1 for these phases conversion ranges. They were better modelled using the

non-normalised conversions, as shown in Figs. 3-4 for PH2 and Fig. 5 for PH1. This is explained by the glycerol decomposition initiating in the middle of PH1 as can be seen from Figs.1-2), indicating that PH1 and PH2 are interconnected by the pure glycerol mass loss. Therefore attempts to treat PH1 and PH2 separately by normalising their conversions between 0 and 1 were expected to fail. For the same reason the kinetic modelling attempted for PH1 is only good in a restricted conversion range due to the limitations of representing the evolution of several compounds with just one set of kinetic parameters. Vice-versa, the modelling of PH2 shown in Fig. 3 indicates the agreement between modelled and experimental conversions is good in the central conversion range (20-70%), dominated by the glycerol reactant. Figure 3 also plots the pure glycerol experimental and modelled conversions with an excellent match. Considering the activation energies of the pure glycerol compared with those of the crude glycerol during PH2, in the ranges 61-74 kJ/mol and 44-50 kJ/mol respectively, together with the fact that higher conversions were clearly seen in Figs 2 and 3 for the crude than for the pure glycerol at a given 'PH2' temperature, indicates clearly that the glycerol in the crude mixture decomposed more readily than pure glycerol. To show this effect more conclusively, the linear fitting yielding the kinetic parameters for the pure glycerol listed in Table 3 was carried out twice for the same heating rate experiment: firstly for the widest range of conversions of linear fit validity, and secondly, in a smaller conversion range equal to that used for fitting the crude glycerol conversions during PH2 at the same heating rate. The discrepancy between pure and crude glycerol decomposition activation energies was observed in both types of fits, with significantly higher values, by 30 kJ/mol for 5 K/min (closest to isothermal conditions) to 10 kJ/mol for 20 K/min. This corroborated that these higher values were not an artefact of using a wider range of conversions and temperatures, but rather reflected a slower pyrolysis chemistry of the pure compared to the crude glycerol during its main decomposition phase.

Conversely, PH3 and PH4 occurred in temperature ranges much higher than that of the pure glycerol decomposition, indicating thermal decomposition thermodynamics and chemistries separate from those of the main component glycerol during PH2. The normalised conversions during PH3 and PH4 were in excellent agreement with their modelled counterparts, which can be seen in Figs 6-7. This further indicated that PH3 and PH4 exhibited independent reaction mechanisms from each other and from those of the previous phases PH1 and PH2. PH3 and PH4 most likely corresponded to distinct families of components undergoing decomposition. The higher activity in evidence in PH2 compared to that of the pure glycerol could then be attributed to PH1-specific components in the crude while those responsible for PH3 and PH4 had no influence on the higher reactivity of PH2. The kinetics of the 3rd and 4th decomposition phases attributed to fatty acid methyl esters cracking and pyrolysis tarry residues were sensitive to the heating rate. As postulated earlier, the crude components responsible for this effect are very likely to be water and methanol. Hence, the TGA experiments of 10% water in crude glycerol and 10% methanol in glycerol were designed to examine this effect. Figure 2 showed that the 10% water-glycerol and the 10% methanol-glycerol exhibited a similar homogeneous catalytic effect as the crude glycerol, their main decomposition being completed at significantly lower temperature than the pure glycerol. We can therefore attribute the lower temperature of onset of PH2 to the presence of both water and methanol. The concept of water-catalysed thermal decomposition reactions in the gas and aqueous phase is not new and forms the basis of many green processes. Although to our knowledge the literature does mention such an effect in glycerol pyrolysis, other oxygenated hydrocarbons have been reported to undergo water-catalysed decomposition such as formic acid decomposition (Chen et al., 2008). Methanol is rarely mentioned as a catalyst of decomposition reactions but rather a reactant in its own right in many organic reactions.

Phase 3 generated activation energies higher than PH2, in the range 77-117 kJ/mol, listed

in Table 5 which, from the FTIR analysis were attributable to the cracking of fatty acid methyl esters and to that of glycerol pyrolysis residue as well as other crude glycerol impurities. Despite finding that the activation energy varied significantly with the heating rate for this phase, the actual conversion curves were very quasi-superimposable for the 10, 15 and 20 K/min heating rates. For all the heating rates, Fig. 6 shows that the calculated conversions were able to reproduce extremely well the experimental conversions of PH3, in the large (normalised) conversion range 0-90 wt%, corroborating the hypothesis of a separate mechanism to those of PH1 and PH2. Phase 4 (PH4) was then modelled with even higher activation energies, listed in Table 6, in the range 229-325 kJ/mol. Local spurious mass fluctuations were registered by the TGA during this phase and were subsequently eliminated from the data for the purpose of the kinetic modelling. Nevertheless, Fig. 7 shows that despite these small gaps in the data, the modelled and experimental conversions for PH4 were in very good agreement. Only the highest conversions showed a discrepancy between calculated and experimental conversions, as would be expected from mass transfer limitations. In the modelling of PH4, the best mechanism function was found to be the 3-D diffusion model as opposed to the power law found for PH1-3. This has two effects: firstly, the diffusion models tend to generate activation energies roughly twice as large as the other models such as power law or reaction order; secondly, this diffusion driven mechanism could arise from layers of intermediate tarry products which would offer a mass transfer resistance to the progress of the pyrolysis reactions. The latter would explain the sensitivity of kinetic parameters of PH4 to the heating rate. In support of this theory, it was observed that in the FTIR spectrum during PH4 the C-C and C=C peaks became more prominent to the detriment of the CO₂ peak, consistent with tar thermal decomposition, leaving coke and ash behind.

3.5. Effect of heating rate

It can be observed from Tables 3-6 that the values of kinetic parameters such as E and A can be different for the four heating rates, in particular for PH3 and PH4, indicating the thermal decomposition of crude glycerol may depend on the experimental conditions. As the heating rate is increased, the maximum mass loss and/or maximum rate of decomposition shift to higher temperatures. This is attributed to the variations in the rate of heat transfer with the change in the heating rate and the short exposure time to a particular temperature at high heating rates, as well as the effect of the kinetics of decomposition. In pyrolysis experiments of pure compounds, heating rate-independent kinetic parameters may be derived using a small range of small heating rates (e.g. 3, 6 and 9 K min⁻¹) according to the numerical methods outlined in Rotaru et al (2007). In the present study where crude glycerol decomposition was modelled via four separate phases, and where larger heating rates were employed, none of these methods were able to generate kinetic parameters that were heating rate-independent.

3.6. Discussion relevant steam reforming of crude glycerol

To conclude the modelling of the four phases of crude glycerol pyrolysis in the light of its potential use as catalytic steam reforming feedstock for production of hydrogen, it is expected that the catalytic steam reforming of crude glycerol generated by manufacturers of biodiesel may be more challenging than that of the pure glycerol. Pure glycerol has a single, well defined narrow range of thermal decomposition, leaving little residue, and therefore offers relatively easy means of conducting steam reforming with little tar or coking. Crude glycerol exhibits a much wider temperature range of thermal decomposition, generating relatively stable residues above 501 K, as reflected by the presence of phase 3 and spanning over 200 K. In addition, in the lower temperature pyrolysis stages, physical phenomena such as vapourisation and chemical

reactions are blurred, generating methane and other hydrocarbon gases by the end of the first phase of the crude decomposition (ca 360 K). Methane requires high temperatures of steam reforming for full conversion to H₂ to be achieved. The residues of the main decomposition of the crude glycerol are much harder to eliminate via thermal means only, as reflected by the presence of the 4th phase of crude glycerol pyrolysis initiating above 760K, and leaving ca. 5% mass residue above 1100K. This easily-formed tarry residue, is likely to offer major impediments to crude glycerol catalytic steam reforming. Ways of avoiding its formation using, for instance, appropriate catalysis routes using for instance a zeolite such as ZSM-5 in the heating zones upstream of the reforming catalyst are therefore recommended.

4. Conclusion

Thermal decomposition of crude glycerol is expected to play an important role in the steam-reforming process. In this paper, the pyrolysis of the crude glycerol from a bio-refinery was studied by thermogravimetry coupled with Fourier transform infrared spectroscopy to shed light on its thermal decomposition mechanism. The pyrolysis of the crude glycerol by-product of a biodiesel production process exhibited four phases and the main gas components evolving from the reaction included CO₂, H₂O, CH₄, CO, and some organics. Low temperature decomposition of the crude glycerol (phases 1 & 2, temperatures below 500K) yield residues difficult to eliminate via thermal means (phase 3, ending below 774K), with diffusion controlled reactions responsible for the final removal of tars before char is left as a residue (phase 4, below 1123K). An improved iterative Coats-Redfern method was used to evaluate non-isothermal kinetic parameters, and the activation energy and pre-exponential factor were calculated by means of linear regressions. The kinetic modelling revealed that the first two phases of the decomposition possibly exhibited a catalytic effect attributed to water and methanol interactions

with the glycerol, difficult to model in their entirety with single reaction decomposition kinetics, while the third and final phases could be treated independently and could be reproduced very well by different models over entire range.

Acknowledgments

The UK's Engineering and Physical Sciences Research Council is gratefully acknowledged for the funding of this work through grant EP/F027389/1. Our thanks to D1 Oils for providing crude glycerol and to MSc students Line Poinel and Neil Bateman for experimental work on the TGA-FTIR.

References

- Adhikari, S., Fernando, S.D., Gwaltney, S.R., To, S.D.F., Bricka, R.M. Steele, P.H., Haryanto, A., 2007. Athermodynamic analysis of hydrogen production by steam reforming of glycerol. *International Journal of Hydrogen Energy* 32, 2875-2880.
- Adhikari, S., Fernando, S.D., To, S.D.F., Bricka, R.M. Steele, P.H., Haryanto, A., 2007. Conversion of glycerol to hydrogen via a steam reforming process over nickel catalysts. *Energy & Fuels* 22, 1220-1226.
- Ahmaruzzaman, M., Sharma, D.K., 2005. Non-isothermal kinetic studies on co-processing of vacuum residue, plastics, coal and petrocrop. *J. Anal. Appl. Pyrolysis* 73, 263–275.
- Buhler, W., Dinjus, E., Ederer, H.J., Kruse, A., Mas, C., 2002. Ionic reactions and pyrolysis of glycerol as competing reaction pathways in near- and supercritical water. *Journal of Supercritical Fluids* 22, 37–53.
- Chen, H-Ts, Chang, J.-G., Chen, H.-L. Computational study on the decomposition of formic acid catalyzed by (H₂O)_x, x=0-3: Comparison of the gas-phase and aqueous-phase results. *Journal of Physical Chemistry A*, 112, 35, 8093-8099.

- Coats, A.W. and Redfern, J.P., 1964. Kinetic parameters from thermogravimetric data. *Nature* 201, 68-69.
- Czernik, S., French, R., Feik, C., Chornet, E, 2002. Hydrogen by catalytic steam reforming of liquid byproducts from biomass thermoconversion process. *Ind. Eng. Chem. Res.* 41, 4209-4215.
- Dupont, V., Ross, A.B., Hanley, I., Twigg, M.V., 2007. Unmixed steam reforming of methane and sunflower oil: a single reactor process for H₂-rich gas. *International Journal of Hydrogen Energy* 32, 67-79.
- Douette, A.M.D., Turn, S.Q., Wang, W., Keffer, V.I., 2007. Experimental investigation of hydrogen production from glycerin reforming. *Energy & Fuels* 21, 3499-3504.
- Dauenhauer, P.J., Salge, J.R., Schmidt, L.D., 2006. Renewable hydrogen by autothermal steam reforming of volatile carbohydrates. *Journal of Catalysis* 244, 238-247.
- Dou, B., Lim, S., Kang, P., Hwang, J., Song, S., Yu, T.-U., Yoon, K.-D., 2007. Kinetic study in modeling pyrolysis of refuse plastic fuel. *Energy & Fuels* 21, 1442-1447.
- Gao, L., Sun, G., Kawi, S., 2008. A study on methanol steam reforming to CO₂ and H₂ over the La₂CuO₄ nanofiber catalyst. *Journal of Solid State Chemistry* 181, 7-13.
- Ma, F., Hanna, M.A., 1999. Biodiesel production: a review. *Bioresource Technology* 70, 1-15.
- Press, W.H., Teukolsky, S.A., Vetterling, W.T., Flannery, B.P., 1992. *Numerical Recipes in Fortran 7: the art of scientific computing*, Cambridge University Press.
- Ranjbar M. and Pusch, G., 1991. Pyrolysis and combustion kinetics of crude oils, asphaltenes and resins in relation to thermal recovery processes. *Journal of Analytical and Applied Pyrolysis*, 20, 185-196.
- Rotaru, A., Moanta, A., Salageanu, I., Budrugaec, P., and Segal, E., 2007. Thermal decomposition kinetics of some aromatic azomonoethers. Part I. Decomposition of

- 4-[(4-chlorobenzyl)oxy]-4'-nitro-azobenze. *Journal of Thermal Analysis and Calorimetry*, 87, 2, 395-400.
- Slinn, M., Kendall, K., Mallon, K., Andrews, J., 2008. Steam reforming of biodiesel by-product to make renewable hydrogen. *Bioresource Technology* 99, 5851-5858
- Stein, Y.S., Antal Jr., M.J., Jones Jr., M., 1983. A study of the gas-phase pyrolysis of glycerol. *Journal of Analytical and Applied Pyrolysis* 4, 283-296.
- Sun, Y., Li, S., 2008. The effect of nitrate esters on the thermal decomposition mechanism of GAP. *Journal of Hazardous Materials* 154, 112-117.
- Tapanes, N.C.O., Aranda, D.A.G Mesquita Carneiro, J.W.D., Antunes, O.A.C., 2008. Transesterification of *Jatropha curcas* oil glycerides: Theoretical and experimental studies of biodiesel reaction. *Fuel* 87, 2286-2295.
- Urbanovici, E., Popescu, C. and Segal, E., 1999. Improved iterative version of the Coats-Redfern method to evaluate non-isothermal kinetic parameters. *Journal of Thermal Analysis and Calorimetry* 58, 683-700.
- Valliyappan, T., Bakhshi, N.N., Dalai, A.K., 2008. Pyrolysis of glycerol for the production of hydrogen or syn gas. *Bioresource Technology* 99, 4476-4483.
- Wu, R., Lee, D., Chang, C., Shie, J., 2006. Fitting TGA data of oil sludge pyrolysis and oxidation by applying a model free approximation of the Arrhenius parameters *J. Anal. Appl. Pyrolysis* 76, 132-137
- Yan, R., Yang, H., Chin, T., Liang, D., Chen, H., Zheng, C., 2005. Influence of temperature on the distribution of gaseous products from pyrolyzing palm oil wastes. *Combustion and Flame* 142, 24-32.
- Zhang, B., Tang, X., Li, Y., Xu, Y., Shen, W., 2007. Hydrogen production from steam reforming of ethanol and glycerol over ceria-supported metal catalysts. *International Journal of Hydrogen Energy* 32, 2367-2373.

Table 1. TGA results of crude glycerol.

		Heating rate (K/min)	5	10	15	20
Phase 1 (PH1)	Mass loss (%)		15	13	12	10
	Initial mass loss temperature (K)		322	341	343	343
	Maximum mass loss temperature (K)		357	369	375	373
	Final mass loss temperature (K)		426	437	438	440
Phase 2 (PH2)	Mass loss (%)		67	68	67	69
	Initial mass loss temperature (K)		426	437	438	440
	Maximum mass loss temperature (K)		476	512	528	528
	Final mass loss temperature (K)		501	525	543	548
Phase 3 (PH3)	Mass loss (%)		10.8	10.9	12.7	10.2
	Initial mass loss temperature (K)		501	528	543	548
	Maximum mass loss temperature (K)		708	735	739	742
	Final mass loss temperature (K)		760	774	773	773
Phase 4 (PH4)	Mass loss (%)		4.3	3.8	3.7	5.8
	Initial mass loss temperature (K)		760	766	773	773
	Maximum mass loss temperature (K)		973	983	996	1023
	Final mass loss temperature (K)		1123	1123	1123	1123

Table 2. TGA results of pure glycerol.

Heating rate (K/min)	5	10	15	20
Mass loss (%)	95	94	94	93
Initial mass loss temperature (K)	423	428	435	453
Maximum mass loss temperature (K)	439	441	523	529
Final mass loss temperature (K)	503	510	556	553

Table 3. Kinetic parameters found using the power law model ($g(\alpha)=\alpha^{-m}$, $m=1$) in PH2 of the pyrolysis of crude glycerol, and in the single phase of the pyrolysis of pure glycerol, for the four heating rates.

β (K/min)	r	Datapoints	Fit α range	E (kJ/mol)	A (s^{-1})	
Crude	5	0.999352	486	0.250-0.756	44.17 ± 1.21	84 ± 607
	10	0.999621	252	0.225-0.703	46.43 ± 1.73	188 ± 1440
	15	0.999134	204	0.191-0.695	44.06 ± 1.57	117 ± 1968
	20	0.999499	113	0.243-0.712	50.62 ± 3.06	692 ± 4219
Pure	5	0.999273	957	0.034-0.900	68.96 ± 0.60	$(45.3 \pm 0.8) \times 10^3$
	5	0.999687	326	0.250-0.760	74.21 ± 3.13	$(183.8 \pm 2) \times 10^3$
	10	0.999291	491	0.030-0.706	63.12 ± 0.73	$(14.2 \pm 1.5) \times 10^3$
	10	0.997249	202	0.225-0.703	61.80 ± 2.91	$(10.2 \pm 2.5) \times 10^3$
	15	0.999400	325	0.042-0.949	67.81 ± 1.00	$(41.6 \pm 2.6) \times 10^3$
	15	0.999983	136	0.191-0.691	71.30 ± 3.94	$(100 \pm 6) \times 10^3$
	20	0.999768	167	0.030-0.318	59.95 ± 1.58	$(8.2 \pm 3.6) \times 10^3$

Table 4. Kinetic parameters found using the power law model ($g(\alpha)=\alpha^{-m}$, $m=1$) in PH1 of the pyrolysis of crude glycerol.

β (K/min)	r	Datapoints	Fit α range	E (kJ/mol)	A (s^{-1})
5	0.988809	602	0.007-0.08	27.65 ± 0.36	2.71 ± 317
10	0.991840	419	0.006-0.08	24.89 ± 0.35	0.989 ± 565
15	0.956824	343	0.006-0.08	34.80 ± 0.35	39.8 ± 1184
20	0.962685	337	0.006-0.08	33.57 ± 0.31	36.3 ± 1504

Table 5. Kinetic parameters found using the power law model ($g(\alpha)=\alpha^{-m}$, $m=1$) in PH3 of the pyrolysis of crude glycerol. The conversion for the fit was normalized to [0-1] for the range indicated.

β (K/min)	r	Datapoints	Fit α range	E (kJ/mol)	A (s^{-1})
5	0.992255	1559	0.882-0.934	77.5 ± 0.4	406 ± 840
10	0.994047	669	0.894-0.964	91.8 ± 1.0	$(5.54 \pm 2.18) \times 10^3$
15	0.999538	379	0.873-0.944	117.6 ± 1.8	$(641.2 \pm 4.8) \times 10^3$
20	0.998646	274	0.862-0.927	103.0 ± 1.7	$(79.5 \pm 5.5) \times 10^3$

Table 6 Kinetic parameters found using the 3D-diffusion model (Jander Equation $g(\alpha) = (1 - (1 - \alpha)^{1/3})^2$) in PH4 of the pyrolysis of crude glycerol. The conversion for the fit was normalized to [0-1] for the range indicated.

β (K/min)	r	Datapoints	Fit α range	E (kJ/mol)	A (s^{-1})
5	0.994559	471	0.9723-0.9822	229.4 ± 1.0	$2.8501 \times 10^8 \pm 8.7 \times 10^3$
10		Too many spikes in TGA data: too poor to model			
15	0.997726	602	0.9664-0.9901	324.7 ± 3.3	$3.3858 \times 10^{13} \pm 1.5 \times 10^4$
20	0.993898	536	0.9474-0.9865	304.2 ± 2.8	$9.5748 \times 10^{11} \pm 7 \times 10^4$

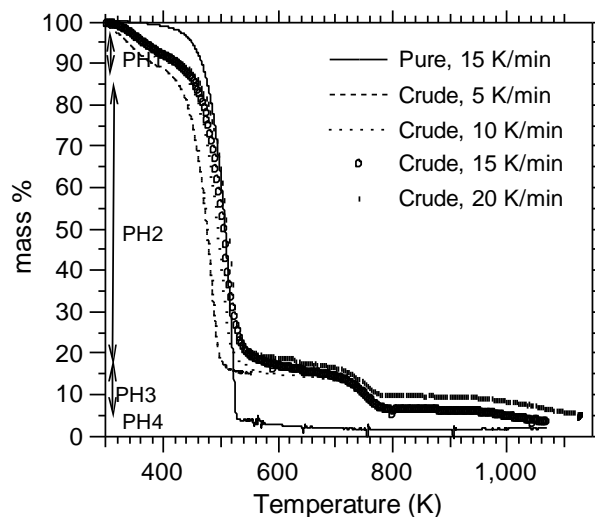


Figure 1. TGA mass loss curves of pure glycerol with 15K/min, and of crude glycerol with 5, 10, 15 and 20 K/min heating rates. The four phases of the pyrolysis of the crude glycerol are indicated as PH1-PH4.

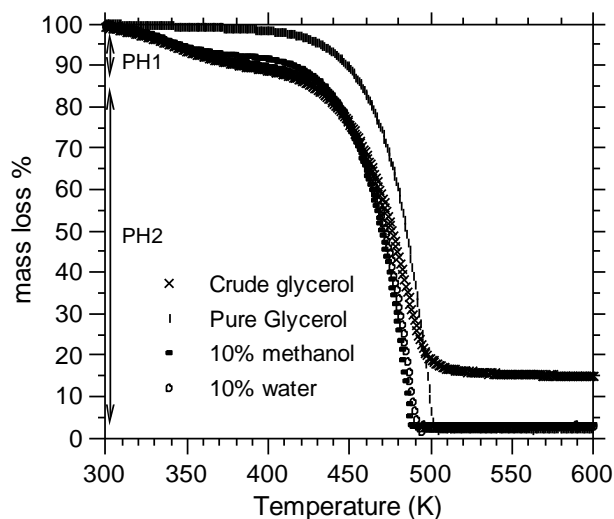


Figure 2. TGA mass loss curves at 5 K min⁻¹ of crude glycerol, pure glycerol, 10% water in pure glycerol, 10% methanol in pure glycerol.

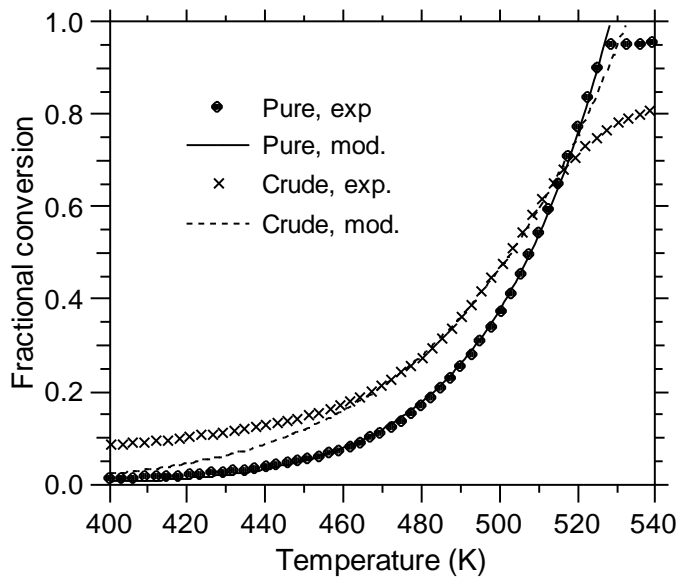


Figure 3. Experimental and modelled conversions of 2nd phase of the pyrolysis (PH2) of pure and crude glycerol at 15 K/min. Experimental points shown with a density of 1 in 10. Modelled curves use the kinetic parameters in Table 3.

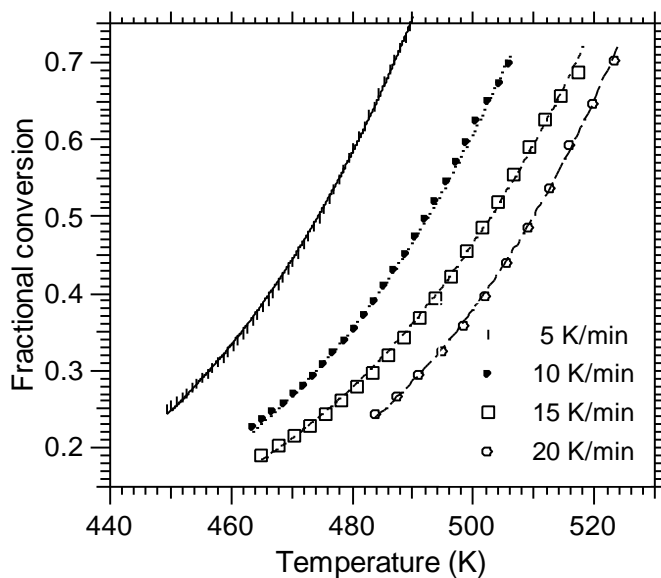


Figure 4. Experimental (scatter points) and modelled (lines) conversions of 2nd phase of the pyrolysis (PH2) of crude glycerol with various heating rates. Experimental points are shown with a density of 1 in 10. Modelled curves use the kinetic parameters in Table 3.

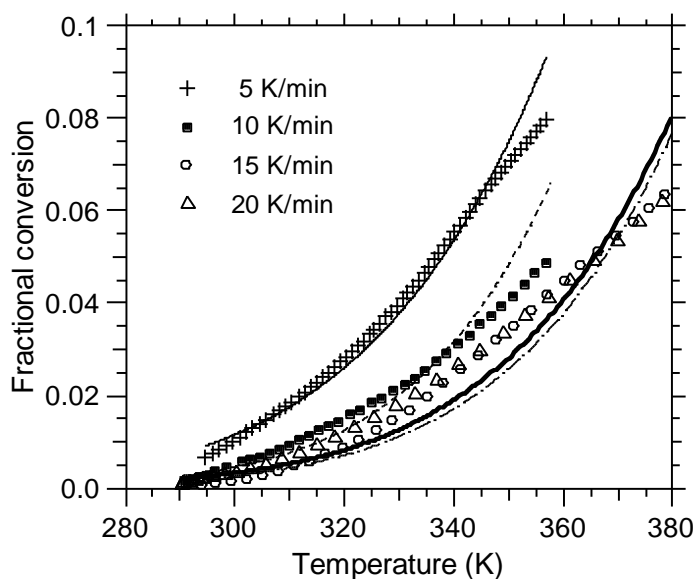


Figure 5. Experimental (scatter points) and modelled (lines) conversions for 1st phase of the pyrolysis (PH1) of crude glycerol. Experimental points are shown with a density of 1 in 10. Kinetic parameters used in the modelled curves are in Table 4.

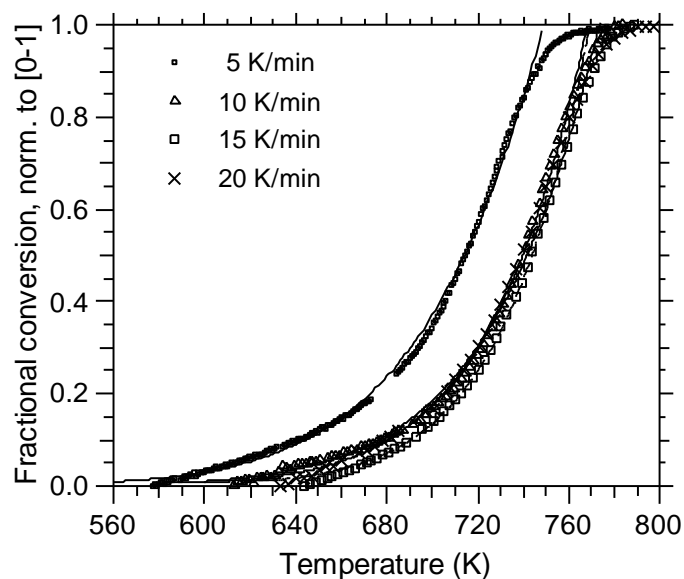


Figure 6. Experimental (scatter points) and modelled (lines) conversions, normalised for 0-1 for conversion range given in Table 1 for 3rd phase of the pyrolysis (PH3) of crude glycerol. Experimental points are shown with a density of 1 in 10. Kinetic parameters used in the modelled curves are in Table 5.

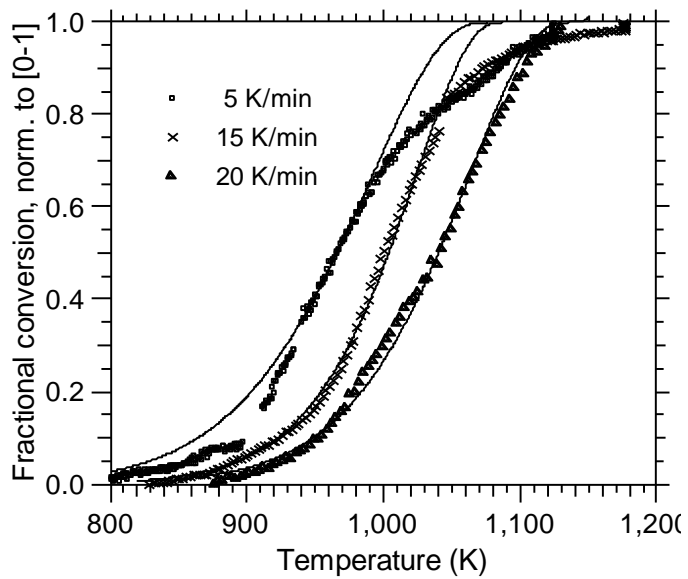


Figure 7 Experimental (scatter points) and modelled (lines) conversions, normalised for 0-1 for conversion range given in Table 2 for 4th phase of the pyrolysis (PH4) of crude glycerol. Experimental points are shown with a density of 1 in 10. Kinetic parameters used in the modelled curves are in Table 6.